

ChemComm

Accepted Manuscript



This is an *Accepted Manuscript*, which has been through the Royal Society of Chemistry peer review process and has been accepted for publication.

Accepted Manuscripts are published online shortly after acceptance, before technical editing, formatting and proof reading. Using this free service, authors can make their results available to the community, in citable form, before we publish the edited article. We will replace this *Accepted Manuscript* with the edited and formatted *Advance Article* as soon as it is available.

You can find more information about *Accepted Manuscripts* in the [Information for Authors](#).

Please note that technical editing may introduce minor changes to the text and/or graphics, which may alter content. The journal's standard [Terms & Conditions](#) and the [Ethical guidelines](#) still apply. In no event shall the Royal Society of Chemistry be held responsible for any errors or omissions in this *Accepted Manuscript* or any consequences arising from the use of any information it contains.

COMMUNICATION

Thermodynamics of halogen bonded monolayer self-assembly at the liquid-solid interface

Cite this: DOI: 10.1039/x0xx00000x

W. Song^{ab}, N. Martsinovich^d, W. M. Heckl^{abc}, and M. Lackinger^{*abc}Received 00th January 2012,
Accepted 00th January 2012

DOI: 10.1039/x0xx00000x

www.rsc.org/

Monolayer self-assembly of a hexabrominated, three-fold symmetric aromatic molecule is studied at the heptanoic acid–graphite interface. Thermodynamical insights are obtained from an adapted Born-Haber cycle that is utilized to derive the overall enthalpy change including solvent effects. Comparison with theoretical entropy estimates suggests a minor influence of solvation.

Halogen bonds have gained attention in crystal engineering, supramolecular self-assembly, and even computer aided drug design.¹⁻⁴ Halogen bonds are viewed as a separate class of donor-acceptor type interactions that originate in the anisotropic charge distribution around halogen substituents, most importantly Br and I. The so called σ -hole gives rise to a positive electrophilic cap at the opposing pole of the σ -bond that is balanced by a nucleophilic equatorial ring of negative charge.⁵⁻⁷ A halogen bond is formed through a net attraction between the electrophilic cap of the halogen with either the nucleophilic part of a different entity, as for instance the nitrogen electron lone pair, or the nucleophilic ring of another halogen. This characteristics results in directionality and selectivity, whereas the halogen bond strength decreases as the halogen electronegativity increases. Moreover, a single halogen substituent can simultaneously act as both halogen bond acceptor and donor – an important distinction from the in other aspects quite comparable hydrogen bonds. A triangular arrangement of three halogen atoms with three cyclic halogen bonds is a frequently encountered motif both in bulk crystals and on surfaces,^{8, 9} but alternative configurations were similarly reported.¹⁰

Supramolecular self-assembly of halogen bonded systems on surfaces was recently studied by scanning tunneling microscopy (STM) both under ultra-high vacuum^{9, 11, 12} and ambient conditions.^{10, 13-15} Accompanying density functional theory simulations based on experimental structures provided insights into the energetics.^{10, 12, 16} While this is an important first step, a fundamental understanding of self-assembly from solution requires a full thermodynamical assessment, including the role of the solvent. As a model system hexabromotriphenylene (HBTP, cf. Fig. 1) is studied at the heptanoic acid (7A)–graphite interface with the aim to quantify all relevant contributions to ΔG . At the liquid-solid interface, the adsorption energy becomes significantly lowered as

compared to vacuum by the supernatant liquid phase. This important solvent influence is quantified for the proposed model system by applying an adapted Born-Haber cycle derived from sublimation, dissolution, and monolayer binding enthalpy in vacuum.¹⁷

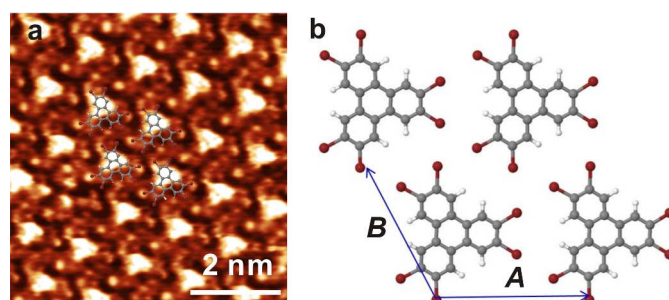


Fig. 1 (a) High resolution STM image of a HBTP monolayer at the 7A-graphite interface. $V_{\text{sample}} = -0.40$ V, $I = 80$ pA, (b) DFT optimized geometry of a free standing HBTP monolayer (grey: carbon, red: bromine, white: hydrogen)

At the 7A–graphite interface HBTP self-assembles into a densely packed structure, a high resolution STM image is presented in Fig. 1a. The lattices of HBTP and graphite are aligned (cf. ESI) and the experimental lattice parameters of $A=B=(12.5 \pm 0.2)$ Å, $\gamma = 59^\circ \pm 2^\circ$ match well with a 5×5 graphite superstructure. Moreover, the absence of a Moiré pattern in these images with pronounced submolecular contrast strongly indicates commensurability. To obtain a detailed structural model, dispersion-corrected DFT simulations of a free-standing HBTP monolayer constrained to a hexagonal lattice were carried out using both empirical dispersion correction (PBE+D) and a van der Waals functional (vdW-DF) (cf. ESI for details). The optimized structure is shown in Fig. 1b. Simulations with unconstrained length of the lattice parameter yield an optimized value of 12.5 Å, i.e. only 1.5 % larger than 12.3 Å of the 5×5 graphite superstructure. The structure belongs to planar space group $p31m$, and all bromines take part in the prototypical triangular cyclic arrangement of halogen bonds with a Br-Br distance of 3.70 Å, in good agreement with literature.¹⁸ Interestingly, the symmetry of high resolution STM images is significantly lower than that of the DFT structure and does not even reflect the three-fold symmetry of HBTP. This clearly indicates an adsorption site of

HBTP with lower local symmetry. Nevertheless, in an overlay STM protrusions can be matched with bromine positions (cf. Fig. 1a). The vdW-DF derived monolayer binding energy per molecule with respect to vacuum of -48.3 kJ/mol is rather small. Compressing the structure to the experimental 5×5 graphite superstructure reduces the binding energy to -43.5 kJ/mol. A very similar binding energy was obtained using PBE+D: -45.5 kJ/mol for the unconstrained free-standing structure and -42.7 kJ/mol for the constrained 5×5 superstructure; VdW-DF was also employed to calculate the total binding energy comprised of molecule-molecule and molecule-surface interactions of HBTP in the adsorbed monolayer on graphite, resulting in $\Delta H_{\text{mono}} = -229.6$ kJ/mol (cf. ESI). Similarly, these calculations yield an adsorption energy for HBTP on graphite of -186.1 kJ/mol per molecule, i.e. the molecule-surface interactions are approximately a factor of 4 larger than the intermolecular interactions.

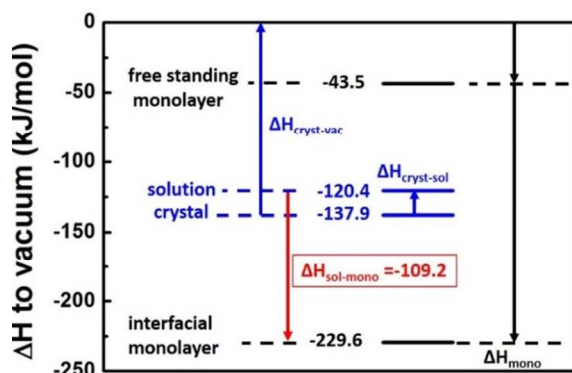


Fig. 2 Enthalpy diagram of the HBTP-7A-graphite system. Black and blue depicted values and arrows correspond to computational and experimental results, respectively. Vertical arrows denote the respective enthalpies.

In the actual experimental situation at the liquid-solid interface HBTP adsorbs from solution, whereby the effective enthalpy difference $\Delta H_{\text{sol} \rightarrow \text{mono}}$ is significantly lowered due to solvent interactions. Since a direct measurement is intricate, $\Delta H_{\text{sol} \rightarrow \text{mono}}$ is indirectly evaluated by combining ΔH_{mono} with experimentally determined sublimation ($\Delta H_{\text{cryst} \rightarrow \text{vac}}$) and dissolution enthalpy ($\Delta H_{\text{cryst} \rightarrow \text{sol}}$) as illustrated in Fig. 2.^{17, 19}

$\Delta H_{\text{cryst} \rightarrow \text{vac}}$ was determined from the temperature dependence of the effusion rate from a Knudsen cell as measured with a Quartz Crystal Microbalance (cf. ESI for details).²⁰ The eigenfrequency decline Δf vs. time t traces are shown in Fig. 3a for crucible temperatures between 225 °C and 270 °C. The rate $\Delta f/\Delta t$ is proportional to the vapour pressure at the respective temperature. The data yield a perfectly linear Van't Hoff plot with a slope corresponding to $\Delta H_{\text{cryst} \rightarrow \text{vac}} = +137.9 \pm 1.6$ kJ/mol.

$\Delta H_{\text{cryst} \rightarrow \text{sol}}$ was determined from the temperature dependence of the solubility as measured by UV-Vis absorption spectroscopy of saturated solutions (cf. ESI for details). Individual absorption spectra are shown in Fig. 3b for temperatures between 22 °C and 54 °C. The absorbance, hence the solubility, increases with temperature indicating endothermic dissolution. The total amount of dissolved HBTP molecules was estimated by integrating over the absorption band from $\lambda = (270..340)$ nm. The data yield a perfectly linear Van't Hoff plot with a slope corresponding to $\Delta H_{\text{cryst} \rightarrow \text{sol}} = +17.5 \pm 0.6$ kJ/mol.

The theoretical (ΔH_{mono}) and both experimental ($\Delta H_{\text{cryst} \rightarrow \text{vac}}$ and $\Delta H_{\text{cryst} \rightarrow \text{sol}}$) enthalpies are compiled in Fig 2 with isolated molecules in vacuum as a common reference state. From this $\Delta H_{\text{sol} \rightarrow \text{mono}}$ of -109.2 kJ/mol can be inferred. In principle, this enthalpy difference

between solution and monolayer may be overestimated due to a possible contribution from dewetting.^{17, 19} Self-assembly of a solute monolayer can require desorption of an initially assembled solvent monolayer, resulting in an enthalpy cost and an entropy gain for dewetting. However, an ordered quasi-static monolayer of 7A has never been observed at room temperature, suggesting that it is thermodynamically unstable ($\Delta G > 0$). Based on the assumption that the differences in interfacial tension between 7A-graphite and 7A-HBTP monolayer are small in comparison to $\Delta H_{\text{sol} \rightarrow \text{mono}}$ contributions of solvent dewetting are not further considered, as they do not significantly affect ΔG .

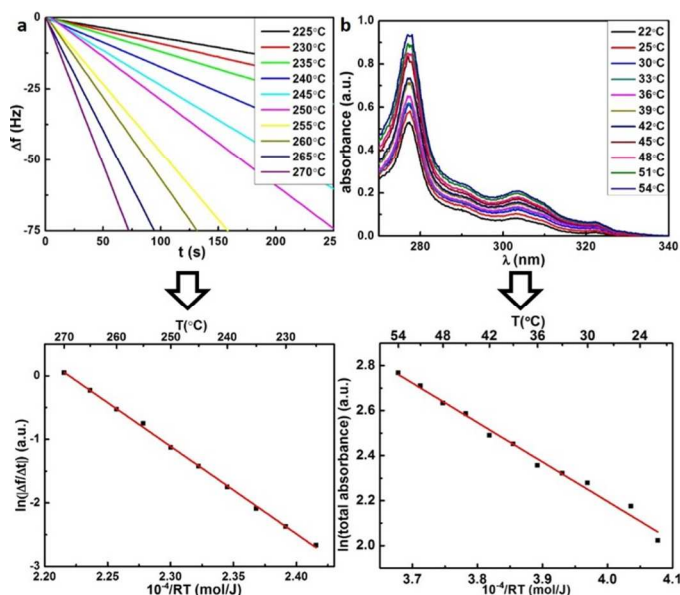


Fig. 3 Experimental determination of $\Delta H_{\text{cryst} \rightarrow \text{vac}}$ and $\Delta H_{\text{cryst} \rightarrow \text{sol}}$ (a) Δf vs. t traces for different crucible temperatures; (b) UV/Vis absorption spectra of saturated solutions for different solution temperatures; the lower panels depict the corresponding Van't Hoff plots; the slopes yield $\Delta H_{\text{cryst} \rightarrow \text{vac}} = (+137.9 \pm 1.6)$ kJ/mol and $\Delta H_{\text{cryst} \rightarrow \text{sol}} = (+17.5 \pm 0.6)$ kJ/mol.

For a complete thermodynamical understanding consideration of entropy contributions is inevitable. Since a direct measurement of ΔS is not possible, we propose an indirect evaluation via the critical concentration c_{crit} , i.e. the lowest solute concentration where self-assembled monolayers are still thermodynamically stable. Since ΔG becomes zero at c_{crit} , the overall entropy change can be determined from: $\Delta S = \Delta H/T$. For HBTP monolayers at the 7A-graphite interface dilution experiments result in $c_{\text{crit}} = 28.8 \pm 3.7$ $\mu\text{mol/L}$ (cf. ESI). Generally, ΔS has several contributions, yet for a rigid molecule such as HBTP translational (S_{trans}) and rotational (S_{rot}) entropy dominate. For molecules within the monolayer S_{rot} and S_{trans} are negligible as compared to the dissolved state, accordingly ΔS can be estimated as the total loss of S_{rot} and S_{trans} . Whitesides et al. propose to estimate S_{rot} with the rigid rotator model, and S_{trans} with the Sackur-Tetrode equation.²¹ Since the latter was originally derived for gases, the solvent influence has to be implicitly taken into account, e.g. by free volume corrections. Table 1 summarizes S_{rot} and S_{trans} contributions evaluated according to this approach (cf. ESI for details). Interestingly, the entropic contribution $-T\Delta S = +111.2$ kJ/mol is almost similar to the absolute value of $|\Delta H_{\text{sol} \rightarrow \text{mono}}| = 109.2$ kJ/mol. This perfect match implies that for HBTP self-assembly no further relevant thermodynamic contributions arise from desolvation. These results stand in vast

contrast to interfacial monolayer self-assembly of 1,4-benzenedicarboxylic acid and stilbene dicarboxylic acid likewise from fatty acid solution.^{17, 19} In both cases $|\Delta H_{\text{sol} \rightarrow \text{monol}}|$ was significantly smaller than $-T\Delta S$ for the adsorption of unsolvated solute molecules. Therefore, it was only possible to explain spontaneous self-assembly by including a favourable entropy contribution from desolvation upon solute adsorption, whereby the released solvent molecules regain S_{trans} and S_{rot} . Dicarboxylic acid solute molecules strongly interact with fatty acid solvent molecules through two-fold hydrogen bonds. Accordingly, solute-solvent and solvent-solvent interactions are of comparable strength in these systems. Owing to the high strengths of carboxylic acid hydrogen bonds, formation of a quasi-static solvation shell can be anticipated for dicarboxylic acids dissolved in fatty acids.

Yet, an entirely different type of solvation can be expected for HBTP in 7A. DFT simulations of HBTP + 7A aggregates provide semi-quantitative values of the solvent-solute interaction strength (cf. ESI). Two different configurations were compared: a structure where simultaneously the 7A hydroxyl forms a hydrogen bond with bromine and the carbonyl oxygen a weak hydrogen bond with a phenyl-hydrogen has a bond strength of -34.1 kJ/mol; an alternative structure with 7A on top of HBTP bound only by dispersion forces has a higher bond strength of -49.8 kJ/mol; The bond strength for both configurations is significantly lower than -67.8 kJ/mol for the hydrogen bonds between carboxylic acids.²² Consequently, for HBTP in 7A, solvent-solvent interactions are significantly stronger than solute-solvent interactions, rendering formation of a strongly bound solvation shell unfavourable. These calculations suggest that the predominant interaction for solvation is van der Waals rather than hydrogen bonding. Also, adsorbed HBTP does not need to lose its “on-top” bound 7A molecules and therefore it can partly retain its solvation shell.

$-T\Delta S_{\text{trans}}(\text{kJ/mol})$	$-T\Delta S_{\text{rot}}(\text{kJ/mol})$	$-T\Delta S(\text{kJ/mol})$
+66.3	+44.9	+111.2

Table 1. Estimation of entropy contributions of HBTP in 7A to ΔG . The entropies are evaluated for c_{crit} at $T = 298 \text{ K}$. (cf. ESI for details).

In conclusion, HBTP self-assembles into densely packed monolayers at the 7A-graphite interface, where each bromine forms intermolecular halogen bonds in a prototypical triangular cyclic arrangement. Simulations clearly indicate that by far the largest contribution to the stabilization of the monolayer arises from molecule-surface interactions through π - π bonds between graphite and the aromatic triphenylene core. The overall enthalpy difference for monolayer self-assembly from the supernatant liquid phase was deduced from a Born-Haber cycle. Accordingly, the solvent reduces the binding enthalpy gain to about 50% of the vacuum value, whereas for dicarboxylic acids a significantly more drastic effect was found in previous studies.^{17, 19} Based on a quantitative comparison of the overall enthalpy and entropy changes, we propose that the contributions from dewetting the substrate and stripping the weakly bound solvation shell of the solute cancel each other such that there are no significant net contributions to ΔG . This hypothesis is supported by energetic arguments: 7A-7A solvent-solvent hydrogen bond interactions are markedly stronger than the dispersive 7A-HBTP solvent-solute interactions. The predominant type of solvation is likely to be mediated by the solvent's interaction with the π -system of HBTP which is not fully lost after adsorption.

This profoundly affects ΔG : there is no favourable entropy contribution due to desolvation; since the intermolecular halogen bonds are comparatively weak, strong molecule-surface interactions are required to render self-assembly of halogen bonded monolayers thermodynamically favourable.

We thank the Nanosystems-Initiative-Munich (NIM) cluster of excellence and the Chinese Scholarship Council for financial support. The University of Sheffield is acknowledged for providing computing resources.

Notes and references

^a Department of Physics, Technische Universität München, James-Frank-Str. 1, 85748 Garching, Germany.

^b Nanosystems-Initiative-Munich and Center for NanoScience (CeNS), Schellingstr. 4, 80799 Munich, Germany.

^c Deutsches Museum, Museumsinsel 1, 80538 Munich, Germany.

^d Department of Chemistry, University of Sheffield, Sheffield S3 7HF, UK.

Electronic Supplementary Information (ESI) available: experimental and simulational details; additional STM data. See DOI: 10.1039/c000000x/

- G. R. Desiraju, *Angew. Chem. Int. Edit.*, 1995, **34**, 2311-2327.
- P. Metrangolo, F. Meyer, T. Pilati, G. Resnati and G. Terraneo, *Angew. Chem. Int. Edit.*, 2008, **47**, 6114-6127.
- Y. X. Lu, T. Shi, Y. Wang, H. Y. Yang, X. H. Yan, X. M. Luo, H. L. Jiang and W. L. Zhu, *J. Med. Chem.*, 2009, **52**, 2854-2862.
- M. Kolar, P. Hobza and A. K. Bronowska, *Chem. Commun.*, 2013, **49**, 981-983.
- P. Politzer, P. Lane, M. C. Concha, Y. Ma and J. S. Murray, *J. Mol. Model.*, 2007, **13**, 305-311.
- T. Clark, M. Hennemann, J. S. Murray and P. Politzer, *J. Mol. Model.*, 2007, **13**, 291-296.
- P. Politzer, J. S. Murray and M. C. Concha, *J. Mol. Model.*, 2008, **14**, 659-665.
- E. Bosch and C. L. Barnes, *Cryst. Growth. Des.*, 2002, **2**, 299-302.
- H. Walch, R. Gutzler, T. Sirtl, G. Eder and M. Lackinger, *J. Phys. Chem. C*, 2010, **114**, 12604-12609.
- R. Gutzler, O. Ivasenko, C. Fu, J. L. Brusso, F. Rosei and D. F. Perepichka, *Chem. Commun.*, 2011, **47**, 9453-9455.
- J. K. Yoon, W.-j. Son, K.-H. Chung, H. Kim, S. Han and S.-J. Kahng, *J. Phys. Chem. C*, 2011, **115**, 2297-2301.
- K.-H. Chung, J. Park, K. Y. Kim, J. K. Yoon, H. Kim, S. Han and S.-J. Kahng, *Chem. Commun.*, 2011, **47**, 11492-11494.
- Q. Chen, T. Chen, X. Zhang, L.-J. Wan, H.-B. Liu, Y.-L. Li and P. Stang, *Chem. Commun.*, 2009, 3765-3767.
- R. Gutzler, C. Fu, A. Dadvand, Y. Hua, J. M. MacLeod, F. Rosei and D. F. Perepichka, *Nanoscale*, 2012, **4**, 5965-5971.
- J. C. Russell, M. O. Blunt, J. M. Garfitt, D. J. Scurr, M. Alexander, N. R. Champness and P. H. Beton, *J. Am. Chem. Soc.*, 2011, **133**, 4220-4223.
- A. R. Voth, P. Khoo, K. Oishi and P. S. Ho, *Nat. Chem.*, 2009, **1**, 74-79.
- W. Song, N. Martsinovich, W. M. Heckl and M. Lackinger, *J. Am. Chem. Soc.*, 2013, **135**, 14854-14862.
- E. Bosch and C. L. Barnes, *Cryst. Growth. Des.*, 2002, **2**, 299-302.
- W. Song, N. Martsinovich, W. M. Heckl and M. Lackinger, *Phys. Chem. Chem. Phys.*, 2014, **16**, 13239-13247.
- R. Gutzler, W. M. Heckl and M. Lackinger, *Rev. Sci. Instrum.*, 2010, **81**, 015108.
- M. Mammen, E. I. Shakhnovich, J. M. Deutch and G. M. Whitesides, *J. Org. Chem.*, 1998, **63**, 3821-3830.
- G. Allen, J. G. Watkinson and K. H. Webb, *Spectrochim. Acta*, 1966, **22**, 807-814.